Noncyclic Berry phase and scalar Aharonov-Bohm phase for the spin-redirection evolution in an atom interferometer

Atsuo Morinaga* and Kota Nanri
Faculty of Science and Technology, Tokyo University of Science, 2641 Yamazaki, Noda-shi, Chiba 278-8510, Japan
(Received 16 April 2012; published 6 August 2012)

Using a magnetic-field-insensitive two-photon transition, the phase shift of atomic interference fringes and the frequency shift of the resonance spectrum were examined for a noncyclic rotation of a magnetic field during the interrogation time of an atom interferometer. We observed a phase shift proportional to the rotation angle of the magnetic field when the initial state and the final state were subjected to interference. We confirmed that the phase shift is equivalent to the scalar Aharonov-Bohm phase due to the geometrical potential. On the other hand, we demonstrated that the noncyclic Berry phase defined by the geodesic gauge is measurable using a strategy that the magnetic field rapidly returns to the initial direction during the interrogation time of the atom interferometer.

DOI: 10.1103/PhysRevA.86.022105 PACS number(s): 03.65.Vf, 03.75.Dg, 32.30.Bv, 32.60.+i

I. INTRODUCTION

In 1984, Berry predicted that in a cyclic adiabatic process, in which the slowly time-varying Hamiltonian returns to its original form via a circuit C, a quantum state may acquire a "geometrical" phase factor $e^{i\gamma} = \exp[-im\Omega(C)]$, where m is the spin component and Ω is the solid angle, in addition to the normal "dynamical" phase factor [1]. Since then, many experimental identifications of the Berry phase have been carried out in various fields of physics [2], and the Berry phase has been generalized to nonadiabatic evolution by Aharonov and Anandan [3]. In 1988, Samuel and Bhandari pointed out that the Berry phase appears in a more general context, such as noncyclic evolution [4], on the basis of the work of Pancharatnam [5]. In noncyclic evolution, the initial state and final state are not orthogonal. Samuel and Bhandari insisted that the noncyclic Berry phase between the initial state and final state can be expressed as a line integral, where the contour C is given by the actual evolution from the initial state to the final state and back along any geodesic curve joining the final state to the initial state, since a phase difference does not occur for a line integral along the geodesic curve. The phase difference is clearly a gauge-invariant quantity and measurable. Thus, the noncyclic Berry phase should be given by the area of the foliage enclosed by the locus of rotation and the geodesic curve, as shown in Fig. 1. In 1990, Weinfurter and Badurek reported the first measurements of the noncyclic Berry phase using polarized neutrons and observed a linear increase in phase shift with increasing rotation angle [6]. However, Wagh and Rakhecha indicated that this result was incorrect and proposed a correct method of measurement for a noncyclic SU(2) evolution with interferometry [7] or with polarimetry [8]. Recently, the noncyclic SU(2) evolution has been verified experimentally without ambiguity [9,10]. However, the noncyclic Berry phase for the spin-redirection evolution of a spinning particle has not yet been demonstrated experimentally.

In 2005, we reported a phase shift for a partial rotation of a magnetic field using a two-photon-stimulated Raman atom interferometer, with which two phases for different spin states were compared [11]. The observed phase shift φ for a partial rotation of angle ϕ is given by

$$\varphi = -m\Omega\frac{\phi}{2\pi}, \tag{1}$$

which is the same as that obtained by Weinfurter and Badurek [6]. After that, we showed that the noncyclic Berry phase defined by a geodesic gauge can be deduced from the phase shift measured by another gauge using the rotation of a polarization azimuth of linearly polarized light in a partially wound optical fiber over the surface of a cylinder [12]. Recently, we have demonstrated a clear atomic Berry phase without a dynamical phase shift for a whole turn of the magnetic field at a magic magnetic field using a magnetic-field-insensitive two-photon "clock" transition between the lower $m = -1$ state and the upper $m = 1$ state [13]. Furthermore, we demonstrated that the linear evolution of the Berry phase with time induces a frequency shift of the resonance transition between two eigenstates [14]. This fact means that the Berry phase for a whole rotation can also be interpreted as the scalar Aharonov-Bohm (SAB) effect due to the time-dependent scalar potential [15,16] caused by the linear evolution of the Berry phase with time. When the period for a whole rotation is T,

$$\gamma \equiv -m\Omega = \int_0^T -\frac{m\Omega}{T}dt \equiv \varphi_{\mathrm{SAB}}. \tag{2}$$

Namely, the SAB phase φ_{SAB} for a whole rotation is identical to the Berry phase γ. These recent results show that our result in 2005 might be explained as the SAB phase for the noncyclic evolution of a magnetic field. If this is the case, how we can measure a noncyclic Berry phase defined by geodesic gauge directly?

In this study, we first examine the geometric frequency shift during the rotation of a magnetic field. Next, we confirm the previous phase shift observed for a partial rotation of a magnetic field using a magnetic-field-insensitive two-photon transition and show that a phase shift proportional to the rotation angle is equivalent to a scalar Aharonov-Bohm phase due to the geometrical potential. Finally, we demonstrate a noncyclic Berry phase measured along a geodesic curve by the strategy that the direction of the magnetic field rapidly returns to the initial direction using a magnetic-field-insensitive two-photon transition.

*morinaga@ph.noda.tus.ac.jp

II. PRINCIPLES

A. Noncyclic Berry phase

Let us consider a sphere moving in the direction of a magnetic field with a spinor particle located at its center O, as shown in Fig. 1. We define the rotation axis of the magnetic field as the z axis (polar axis). P is the zenith of the sphere. The magnetic field is initially in the x-z plane and the angle between the magnetic field and the z axis is θ, which is called the semiangle. In this paper, we assume that the magnetic field rotates around the z axis from the initial point to the final point with a rotation angle ϕ. Then the tip of the magnetic field traces an arc AB on the sphere. For a whole rotation ($\phi = 2\pi$), the solid angle is $\Omega = 2\pi(1-\cos\theta)$, while for a partial rotation, the solid angle depends on the gauge, as discussed in Ref. [12]. For example, if we use a gauge fixed at the zenith, the solid angle becomes the area of the spherical triangle connecting A, B, and P, namely, $\Omega = \phi\cos\theta$.

According to Samuel and Bhandari, the Berry phase between the initial state $|\psi(0)\rangle$ at A and the final state $|\psi(t_{\rm B})\rangle$ at B is expressed as the integral

$$\gamma = \oint A_s ds = \oint_C \mathrm{Im}\left\langle \psi(t) \left| \frac{d\psi(t)}{dt} \right\rangle \right/ \langle \psi(t) \mid \psi(t)\rangle\,, \qquad (3)$$

where the closed loop C is given by the actual evolution of $|\psi(t)\rangle$ from $|\psi(0)\rangle$ to $|\psi(t_{\rm B})\rangle$ and back along any geodesic curve joining $|\psi(t_{\rm B})\rangle$ to $|\psi(0)\rangle$ [4]. A great circle passing through both A and B is determined uniquely owing to the geodesic rule, as shown in Fig. 1. The solid angle can be expressed as the area of the foliage, enclosed by the locus of rotation and the geodesic curve. Then, the Berry phase for a partial rotation is given by

$$\gamma(\theta,\phi) = -m \begin{cases} 2\sin^{-1}\left[\frac{\sin(\phi/2)}{\sqrt{1+\tan^2\theta\cos^2(\phi/2)}}\right] - \phi\cos\theta, & 0 \leqslant \phi \leqslant \pi \\ 2\left\{\pi - \sin^{-1}\left[\frac{\sin(\phi/2)}{\sqrt{1+\tan^2\theta\cos^2(\phi/2)}}\right]\right\} - \phi\cos\theta, & \pi \leqslant \phi \leqslant 2\pi. \end{cases} \qquad (4)$$

Therefore, to measure a noncyclic Berry phase, we must add the second operation of the magnetic field back along the geodesic curve from the final point to the initial point to form a cyclic evolution. Next, we must experimentally consider how to operate the direction of the magnetic field along the geodesic curve. We consider that the evolution along the geodesic curve is equivalent to the instantaneous return of the direction of the magnetic field to the initial state.

B. Two-photon atom interferometer

Atom interferometers are composed of two different magnetic quantum states, which are the superposition from the initial ground state at the first $\pi/2$ resonance pulse and are superimposed into the excited state (or the ground state) at the second $\pi/2$ resonance pulse after the interrogation time [17]. The phase difference arising between the two states during the interrogation time is obtained by measuring the population probability of the excited state (or the ground state) after being superimposed. However, there are two essential problems in noncyclic rotation, one of which is the orthogonality between the initial state and the final state, and the other is the dynamical phase shift due to the Zeeman effect.

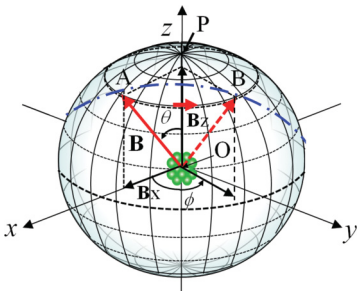

FIG. 1. (Color online) Sphere of the direction of the magnetic field $\boldsymbol{B}$. Atoms are located at the center O. P is zenith of the sphere. The total magnetic field $\boldsymbol{B}$, which is composed of $\boldsymbol{B}_x$ and $\boldsymbol{B}_z$, rotates from A to B with a semiangle θ from $+z$ axis and a rotation angle ϕ. Dot and dashed line is the geodesic curve passing through A and B.

In the noncyclic spin-redirection phase, the magnetic field is rotated during the interrogation time and the state vector is also rotated during this time. In this case, the final state is not orthogonal to the initial state. However, using the above-mentioned atom interferometer, we measure the phase shift with the second excitation pulse in the same direction as the first one. When the state returns to the initial point along the geodesic curve, the noncyclic Berry phase shift between the initial state and the final state is measurable using the same excitation pulse.

In order that no dynamical phase shift is induced by the perturbation of the magnetic field during the interrogation time, we should use a transition frequency between the two states that is insensitive to the magnetic field. The two-photon microwave radio-frequency transition from the $F = 1$, $m_F = -1$ state to the $F = 2$, $m_F = 1$ state is effective, as shown in our previous paper [13].

Figure 2(a) shows an energy diagram of the ground-state hyperfine levels of ^{23}Na with the Zeeman splitting depending on the strength of the magnetic field and the three two-photon transitions. The g factors of the $F = 1$ and $F = 2$ states are $-1/2$ and $1/2$, respectively. According to the Breit-Rabi equation, the resonance frequency $\nu_{-1,1}$ between the $|F = 1, m_F = -1\rangle$ and $|F = 2, m_F = 1\rangle$ states is minimum at $B_0 = 67.7$ μT, which is called the "magic" magnetic field, and it is 762.3 Hz lower than the resonance frequency $\nu_0 = 1.771\,626\,129 \times 10^9$ Hz between the $F = 1$ and $F = 2$ states at zero magnetic field [18]. Therefore, the resonance frequency $\nu_{-1,1}$ is insensitive to the variation of the magnetic

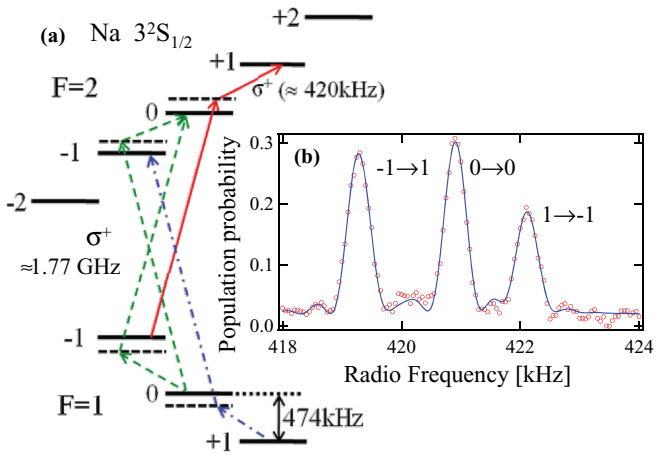

FIG. 2. (Color online) (a) Zeeman splitting of the ground hyperfine state of ^{23}Na under the magnetic field of 67.7 μT, together with two-photon microwave–radio-frequency (MW-rf) transitions. (b) Spectra of the $|1,-1\rangle \rightarrow |2,1\rangle$, $|1,0\rangle \rightarrow |2,0\rangle$, and $|1,1\rangle \rightarrow |2,-1\rangle$ two-photon transitions as a function of radio frequency.

field around B_0. On the other hand, at strengths of the magnetic field B (in the unit of μT) around the magic value, the resonance frequency $\nu_{0,0}$ between the $|1,0\rangle$ and $|2,0\rangle$ states is given by $\nu_0 + 0.2218B^2$ Hz, and the resonance frequency $\nu_{1,-1}$ between the $|1,1\rangle$ and $|2,-1\rangle$ states is given by $\nu_0 - 762.3 + 0.1664(B + B_0)^2$ Hz.

At the magic magnetic field, the Zeeman splitting frequency is 474 kHz. We apply a pulse of microwave (MW) radiation, whose frequency is 420 kHz less than ν_0, along with an rf field of approximately 420 kHz. This two-photon MW-rf transition connects the $|1,-1\rangle$ state to the $|2,1\rangle$ state by $\sigma^+ - \sigma^+$ polarized fields [19]. The three typical spectra of the two-photon transitions plotted against radio frequency are shown in Fig. 2(b).

III. EXPERIMENTAL APPARATUS AND PROCEDURES

Our experimental setup was almost the same as that described in a previous paper [13]. Here, we summarize it briefly. Sodium atoms were trapped in a dual-operated magneto-optical trap (MOT) [20] and cooled by polarization gradient cooling. The temperature of the sodium atoms was approximately 200 μK and the number of trapped atoms was 10^9 with a peak density of 10^{11} atoms/cm^3. A few milliseconds after the release of atoms from the trap, the magnetic field B_x was applied in the x direction. All the atoms were initialized to the $F = 1$ state by optical pumping. The three magnetic sublevels of the $|1,1\rangle$, $|1,0\rangle$, and $|1,-1\rangle$ states were populated with equal population probabilities. Next, the magnetic field B_z was applied in the z direction. The semiangle θ of the total magnetic field from the z axis was $\cos\theta = B_z/\sqrt{B_x^2 + B_z^2}$.

The time-domain atom interferometer was composed of two two-photon MW-rf pulses with pulse widths of 0.8 ms, which were separated by 5 ms. By tuning the radio frequency to approximately 420 kHz, Ramsey fringes with a cycle of 172 Hz were obtained with a visibility of 60% at a constant magnetic field. During the two pulses, the magnetic field B_x was adiabatically rotated in the x-y plane with a constant frequency f (or a period of $T = 1/f$). B_x was adjusted to the magic magnetic-field strength (67.6 ± 0.1 μT), which corresponds to a Larmor frequency of 470 kHz. Magnetic fields along the x and y axes were produced by two mutually orthogonal Helmholtz coils [21]. The coils were driven by alternating currents with a relative phase shift of 90°. The wave forms of the currents were produced by multifunction synthesizers. During the rotation, the amplitude of each alternating current was adjusted so that the Zeeman frequency shifts of the resonance for magnetic-field-sensitive transitions were 67.7 ± 0.1 μT. The rotation frequency used in this study, $f = 200$ Hz, was sufficient to satisfy the adiabatic condition. Finally, the population probability of atoms in the excited state after excitation by the second two-photon pulse was measured by the absorption of a probe laser whose frequency was resonant with the excited state.

IV. RESULTS AND DISCUSSION

A. Frequency shift during rotation

In a previous experiment [14], we confirmed that the center frequency of a spectrum excited by a two-photon pulse with a pulse width longer than the period T of rotation, shifts by $\gamma/(2\pi T)$ due to the linearly evolving Berry phase with time. Here, we examine the shift of the center frequency of a spectrum excited by a pulse with a period shorter than T. The timing diagram of the measurements is shown in Fig. 3(a). The direction of the magnetic field was rotated continuously with a frequency of 200 Hz. The temporal spectrum for the transition between the $|1,-1\rangle$ state and the $|2,1\rangle$ state was measured using a two-photon pulse with a pulse width of 2 ms by shifting the irradiation time of the pulse by 0.5 ms. The center frequency of $\nu_{-1,1}$ is plotted in Fig. 3(b) for semiangles of 76°, 90°, and 104°. The three center frequencies vary sinusoidally. As the frequency for a semiangle of 90° should not be shifted by the evolution of the Berry phase, this sinusoidal shift arises from the Doppler shift due to the rotation of the magnetic field [14]. Therefore, the other two curves involve the same Doppler shift and we can obtain the actual frequency shifts due to the evolution of the Berry phase by extracting the results for 90° from the other results. In this way, the frequency shifts due to the evolution of the Berry phase were obtained, as shown in Fig. 3(c). These results verify that frequency shift due to the Berry phase is also constant to $\gamma/(2\pi T)$ during rotation, although there is still some offset. However, note that the frequency shift of $\nu_{-1,1}$ during rotation is the sum of the frequency shift due to the evolution of the Berry phase and the Doppler shift due to the rotation.

B. Phase shift for noncyclic rotation

In a previous experiment [11], the direction of the magnetic field was partially rotated between two Raman pulses, constituting a Ramsey atom interferometer, and we observed that the phase shift increased proportionally to the rotation angle ϕ under a large dynamical phase shift. We examined whether or not the results could be reproduced using the present two-photon atom interferometer without the dynamical phase shift.

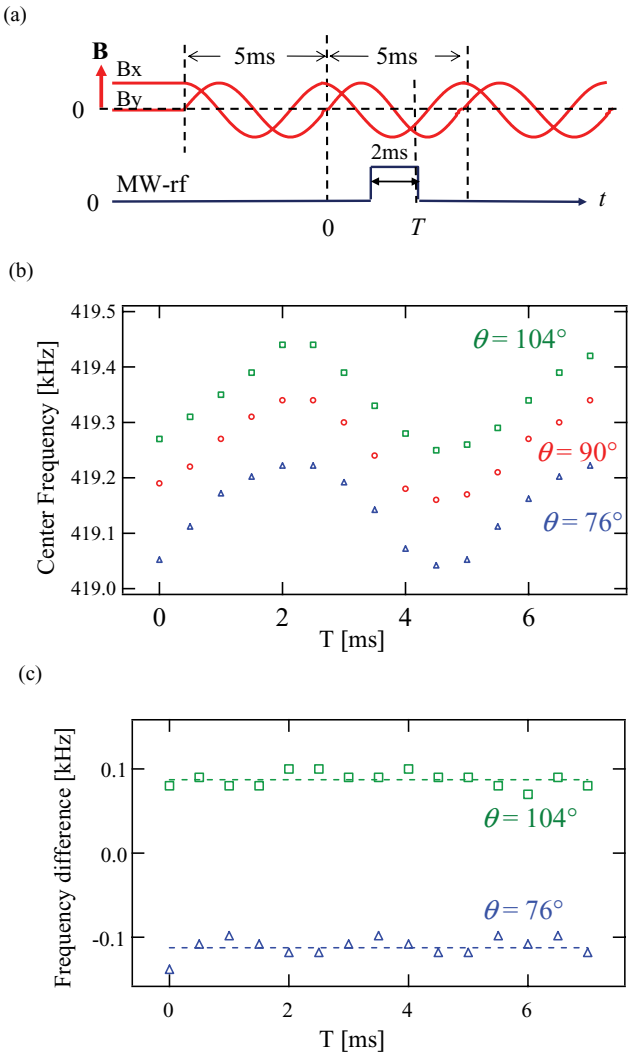

FIG. 3. (Color online) (a) Timing diagram of the irradiation time of pulse under the rotation of the magnetic field. (b) Observed center frequencies for some semiangles versus the irradiation time T. (c) Frequency differences from the center frequency for $\theta = 90°$.

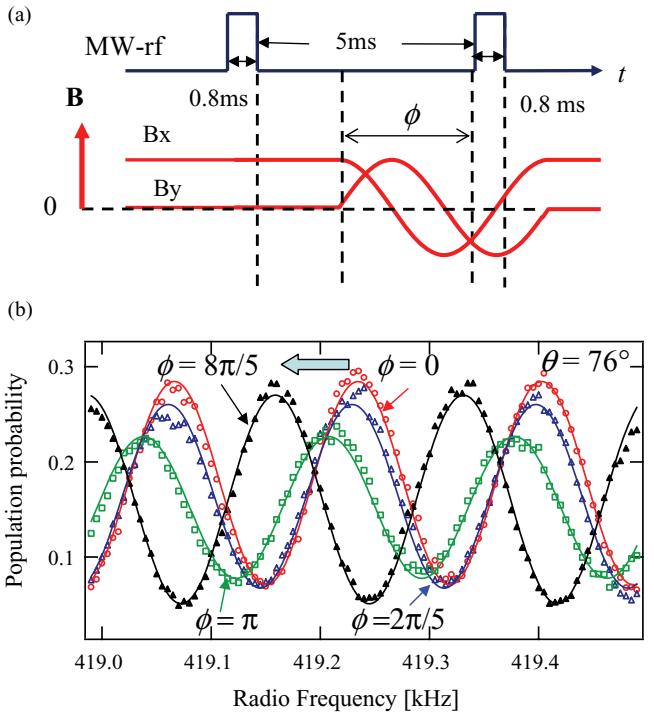

FIG. 4. (Color online) (a) Timing diagram of two two-photon MW-rf pulses and wave forms for magnetic fields of $\boldsymbol{B}_x$ and $\boldsymbol{B}_z$. ϕ is a rotation angle of the magnetic field during two pulses. (b) Observed Ramsey fringes for rotation angles under a semiangle $\theta = 76°$. (○) $\phi = 0$; (△) $\phi = 2\pi/5$; (□)$\phi = \pi$; (▲) $\phi = 8\pi/5$.

We used two two-photon pulses with a pulse width of 0.8 ms, which were separated by 5 ms. During the interrogation time, the direction of the magnetic field was partially rotated by ϕ, as shown in Fig. 4(a). The Ramsey fringes around the resonance frequency obtained for a semiangle of 76° and various rotation angles are shown in Fig. 4(b). The center frequency of the fringes becomes lower, namely, the phase of the fringes is shifted to the positive side, as ϕ increases. In contrast, the phase of the fringes for a semiangle of 104° was shifted to the negative side.

The obtained phase shifts are plotted in Fig. 5(a) for semiangles of 76°, 90°, and 104°. Similarly to in Sec. III A, the phase for a semiangle of 90° is not constant at 0 rad for different rotation angles. Therefore, we subtracted the phase for 90° from the phases for 76° and 104°. The results lie on straight lines, as shown in Fig. 5(b). Thus, the phase shifts are proportional to the angle of rotation ϕ, namely, $\varphi = 2\phi\cos\theta$. As the Berry phase of the $|1,-1\rangle$ and $|2,1\rangle$ states for a whole rotation is $\gamma = 4\pi\cos\theta$, the relation becomes

$$\varphi = \gamma\phi/2\pi. \tag{5}$$

This confirms our previous results. Thus, the solid angle is the area of the spherical triangle enclosed by the arc AB and the great circles PA and PB. Namely, it means the phase was measured using a polar gauge as discussed in Ref. [12].

This result can be also interpreted as the SAB phase due to the geometrical potential, namely, the phase is the time integral of the potential divided by $\hbar$ up to the rotation angle ϕ at time t,

$$\varphi_{\mathrm{SAB}} = 4\pi\cos\theta\frac{t}{T} = 2\phi\cos\theta. \tag{6}$$

Therefore, the phase shift increases proportionally with ϕ during the rotation of the magnetic field. The SAB phase shifts due to the geometric potential are modified by the SAB effect due to the Doppler effect, as seen in Fig. 5(a).

C. Noncyclic Berry phase with rapid return

To measure the noncyclic Berry phase, Samuel and Bhandari proposed that the actual noncyclic evolution is followed by its return along the geodesic curve joining the final state to the initial state. Thus, the line integral along any geodesic curve from the final state to the initial state is zero. However, it will be difficult to rotate the direction of the magnetic field along the geodesic curve connecting the initial and final states experimentally. Instead of a geodesic curve, we assumed a strategy that the direction of the magnetic field rapidly returns to the initial state. Figure 6(a) shows the timing diagram with wave forms for the magnetic-field components B_x and B_y.

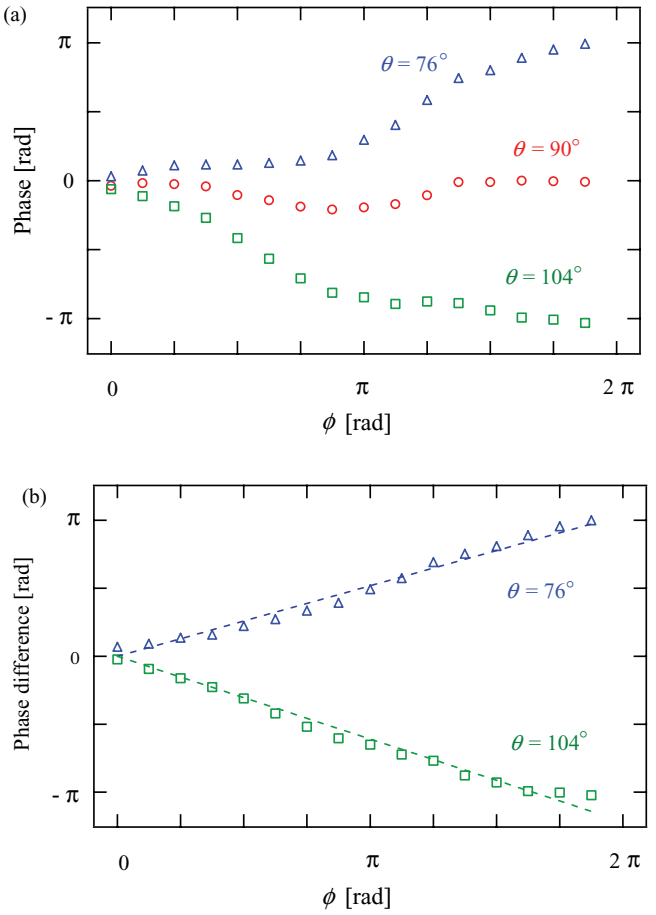

FIG. 5. (Color online) (a) Observed phase shift versus rotation angle for some semiangles. (b) Phase differences from the phase for $\theta = 90^\circ$.

After their evolution, B_x and B_y return to the initial values B_{x0} and By_0, respectively. However, a change of less than 1 μs caused a large ringing, resulting in a marked reduction of the visibility of the fringes. Therefore, a jump with a time constant of 60 μs was used.

The obtained Ramsey fringes for a semiangle of 76° are shown in Fig. 6(b). In contrast to the former experiment, the phase shifts in the negative direction as ϕ increases [cf. Fig. 4(b)]. The obtained phase shifts for various semiangles are summarized in Fig. 7. The phase shift, except for when $\theta = 90^\circ$, changes abruptly from 0 at approximately $\phi = \pi$ and reaches the value at $\phi = 2\pi$:

$$\varphi = \begin{cases} -2m\pi + 4\pi\cos\theta & 0 < \theta < 90^\circ \\ 2m\pi + 4\pi\cos\theta & 90^\circ < \theta < 180^\circ, \end{cases} \tag{7}$$

where m is positive number. Unfortunately, the Ramsey fringes disappeared at $\phi = \pi$, because A and B are connected by plural geodesic curves and fringes interfere destructively. When we supposed $m = 2$, the obtained phase shifts are well described by the curves calculated using Eq. (4) taking the g factor into consideration [13]. The phases for $\theta = 90^\circ$ were almost 0 for all ϕ; however, the calculation for $\theta = 90^\circ$ suggests that the phase jumps by $\pm 4\pi$ at $\phi = \pi$. In the experiment using an optical fiber, we reduced the noncyclic Berry phase from the phase shift measured using the other gauge [12]. The present results

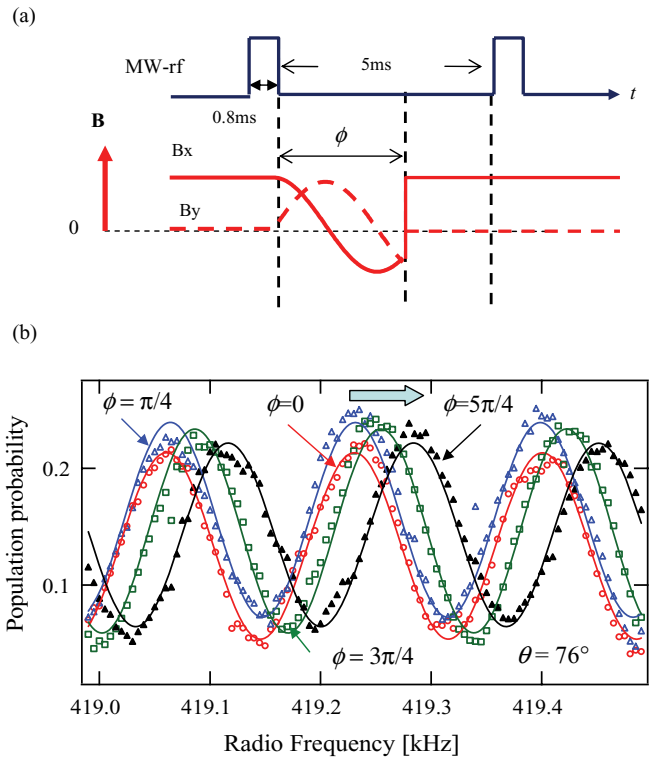

FIG. 6. (Color online) (a) Timing diagram of two two-photon MW-rf pulses and wave forms for magnetic fields of $\boldsymbol{B}_x$ and $\boldsymbol{B}_z$. After rotation of ϕ, the direction of the magnetic field returns to the initial direction rapidly. (b) Observed Ramsey fringes for rotation angles under a semiangle $\theta = 76^\circ$. (○) $\phi = 0$; (△) $\phi = \pi/4$; (□) $\phi = 3\pi/4$; (▲) $\phi = 5\pi/4$.

are in agreement with the theoretical results of Eq. (4), except for the ambiguity of 4π. Therefore, we could demonstrate that the noncyclic Berry phase defined by the geodesic gauge proposed by Samuel and Bhandari can be realized using an atom interferometer by a strategy that the direction of the magnetic field rapidly returns from the final direction to the initial direction after rotation.

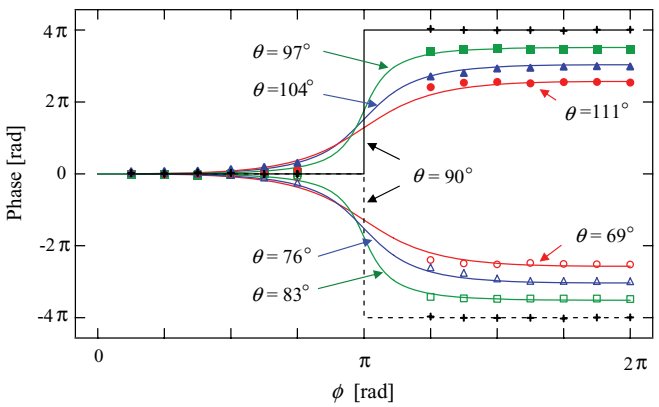

FIG. 7. (Color online) Observed phase for various θ versus rotation angle. For $\phi > \pi$, the experimental values are shifted in 4π for $\theta > \pi/2$ and in -4π for $\theta < \pi/2$. The solid lines are theoretical curves calculated for the noncyclic Berry phase defined by a geodesic gauge.

V. CONCLUSION

Using an atom interferometer formed by a magnetic-field-insensitive two-photon transition between sodium hyperfine levels, the phase shift of interference fringes was investigated under noncyclic rotation of a magnetic field. First, we examined that the geometric frequency shift is constant during a linear rotation of the magnetic field with time. Next, we confirmed the previous phase shift observed for a noncyclic rotation of the magnetic field and showed that the phase shift is proportional to the rotation angle and corresponds to the phase shift measured using a fixed gauge in a direction sphere. It is also equivalent to the scalar Aharonov-Bohm phase due to the linear evolution of the geometrical potential with time. Finally, we demonstrated the measurement of the noncyclic Berry phase along the geodesic curve, whose solid angle is the area of the foliage enclosed by the locus of rotation and the geodesic curve, by a strategy that the direction of the magnetic field rapidly returns to the initial direction during the interrogation time.

ACKNOWLEDGMENTS

We are indebted to Ichiro Inano for his preparation of appropriate wave forms for this experiment. A.M. is grateful to Professor M. Kitano for his profitable discussions of the noncyclic Berry phase.

[1] M. V. Berry, Proc. R. Soc. London A **392**, 45 (1984).
[2] *Geometric Phases in Physics*, edited by A. Shapere and F. Wilczek (World Scientific, Singapore, 1989).
[3] Y. Aharonov and J. Anandan, Phys. Rev. Lett. **58**, 1593 (1987).
[4] J. Samuel and R. Bhandari, Phys. Rev. Lett. **60**, 2339 (1988).
[5] S. Pancharatnam, Proc. Indian Acad. Sci. Sect. A **44**, 247 (1956).
[6] H. Weinfurter and G. Badurek, Phys. Rev. Lett. **64**, 1318 (1990).
[7] A. G. Wagh and V. C. Rakhecha, Phys. Lett. A **197**, 107 (1995).
[8] A. G. Wagh and V. C. Rakhecha, Phys. Lett. A **197**, 112 (1995).
[9] S. Filipp, Y. Hasegawa, R. Loidl, and H. Rauch, Phys. Rev. A **72**, 021602(R) (2005).
[10] J. Klepp, S. Sponar, Y. Hasegawa, E. Jericha, and G. Badurek, Phys. Lett. A **342**, 48 (2005).
[11] A. Morinaga, T. Aoki, and M. Yasuhara, Phys. Rev. A **71**, 054101 (2005).
[12] A. Morinaga, A. Monma, K. Honda, and M. Kitano, Phys. Rev. A **76**, 052109 (2007).
[13] A. Morinaga, K. Toriyama, H. Narui, T. Aoki, and H. Imai, Phys. Rev. A **83**, 052109 (2011).
[14] K. Toriyama, A. Oguchi, and A. Morinaga, Phys. Rev. A **84**, 062103 (2011).
[15] G. Badurek, H. Weinfurter, R. Gähler, A. Kollmar, S. Wehinger, and A. Zeilinger, Phys. Rev. Lett. **71**, 307 (1993).
[16] K. Numazaki, H. Imai, and A. Morinaga, Phys. Rev. A **81**, 032124 (2010).
[17] T. Aoki, K. Shinohara, and A. Morinaga, Phys. Rev. A **63**, 063611 (2001).
[18] D. A. Steck, "Sodium D Line Data," http://steck.us/alkalidata (2008).
[19] K. D. Bonin and T. J. McIlrath, J. Opt. Soc. Am. B **1**, 52 (1984).
[20] H. Tanaka, H. Imai, K. Furuta, Y. Kato, S. Tashiro, M. Abe, R. Tajima, and A. Morinaga, Jpn. J. Appl. Phys. **46**, L492 (2007).
[21] A. Takahashi, H. Imai, K. Numazaki, and A. Morinaga, Phys. Rev. A **80**, 050102(R) (2009).